Article

pubs.acs.org/Biomac

N-Acetylgalactosamine Block-*co*-Polycations Form Stable Polyplexes with Plasmids and Promote Liver-Targeted Delivery

Yogesh K. Dhande,[†] Bharat S. Wagh,[‡] Bryan C. Hall,[§] Dustin Sprouse,[‡] Perry B. Hackett,[§] and Theresa M. Reineke*[,‡]

[†]Department of Chemical Engineering and Materials Science, and Center for Genome Engineering, [‡]Department of Chemistry and Center for Genome Engineering, and [§]Department of Genetics, Cell Biology and Development, and Center for Genome Engineering, University of Minnesota, Minneapolis, Minnesota 55455, United States

Supporting Information

ABSTRACT: The liver is an ideal target for nucleic acid therapeutic applications (i.e., siRNA, gene therapy, and genome editing) due to its ability to secrete proteins into the blood. In this work, we present the first synthesis of a novel monomer derived from *N*-acetyl-D-galactosamine (GalNAc) and its polymerization as a facile route to create multivalent delivery vehicles with exceptional targeting efficiency to asialoglycoprotein receptors (ASGPRs) on liver hepatocytes. A series of cationic diblock GalNAc glycopolymers composed of a GalNAc-derived block of fixed length (n = 62) and cationic 2-aminoethylmethacrylamide (AEMA) blocks of varying lengths (n = 19, 33, and 80) have been synthesized and characterized. In addition, nontargeted control polymers consisting of either glucose or polyethylene glycol-derived neutral blocks with an AEMA cationic block were also created and examined. All polymeric vehicles were able to bind and encapsulate plasmids (pDNA) into polymer−pDNA complexes (polyplexes). The GalNAc-derived polyplexes were colloidally stable and maintained their size over a period of 4 h in reduced-serum cell culture media. The GalNAc-derived homopolymer effectively inhibited the uptake of Cy5-labeled asialofetuin (a natural ligand of ASGPRs) by cultured hepatocyte (HepG2) cells at lower concentrations (IC_{50} = 20 nM) than monomeric GalNAc (IC_{50} = 1 mM) and asialofetuin (IC_{50} = 1 μM), suggesting highly enhanced ASGPR binding due to multivalency. These polymers also showed cell type-specific gene expression in cultured cells, with higher protein expression in ASGPR-presenting HepG2 than HeLa cells, which lack the receptor. Biodistribution studies in mice show higher accumulation of pDNA and GalNAc-derived polymers in the liver compared with the glucose-derived nontargeted control. This study demonstrates the first facile synthesis of a multivalent GalNAc-derived block copolymer architecture that promotes enhanced delivery to liver and offers insights to improve targeted nanomedicines for a variety of applications.

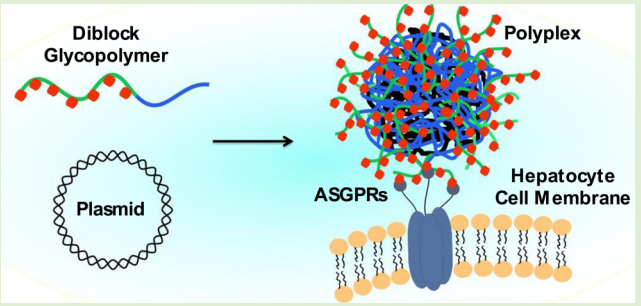

INTRODUCTION

Tissue-specific delivery offers promise to reduce toxicity and immunogenicity as well as improve efficacy of numerous therapeutics ranging from small molecule drugs to proteins and nucleic acids.[1−3] Recent advances in the field of gene therapy such as the clinical approval of Glybera[4] by the European Commission and numerous ongoing clinical trials[5,6] forecast the great potential of gene and RNAi-based therapeutics, but efficient delivery of nanomedicines to specific tissues remains a challenge. The liver is a widely studied target for nucleic acid therapies due to its large size, regenerative ability, and role in the production and secretion of serum proteins into the blood, which has huge potential for permanent therapeutic intervention.[7] Liver-targeted therapies for the treatment of inherited disorders such as hemophilia and mucopolysaccharidoses using viral and nonviral vectors have been promising,[8] but are often limited by either immunogenicity or low efficacy.[9−12] Receptor-mediated targeting has shown encouraging results in delivering siRNA to the liver,[13] but few studies have shown efficient plasmid delivery in whole animals.[14] Indeed, new delivery vehicles are needed to address these challenges and aid rapid advancement of new therapies toward the clinic.

Nonviral vectors, such as cationic polymers, have emerged as a promising class of gene delivery vehicles because of their safety, low immunogenicity, and low cost of production compared to viruses.[15,16] Cationic polymers such as polyethylenimine (PEI),[17] poly(L-lysine),[18] poly((2-dimethylamino) ethyl methacrylate),[19,20] and poly(2-aminoethylmethacrylamide)[21] condense DNA into nanoparticles, called polyplexes, that are efficiently taken up by cells through either caveolae or clathrin-mediated endocytic pathways.[22−25] However, this success in vitro has yet to be translated into clinical therapies due to several challenges.[26] Principally, in the presence of aqueous ions and other charged species, polyplexes tend to

Received: November 17, 2015
Revised: January 4, 2016

DOI: 10.1021/acs.biomac.5b01555
Biomacromolecules XXXX, XXX, XXX−XXX

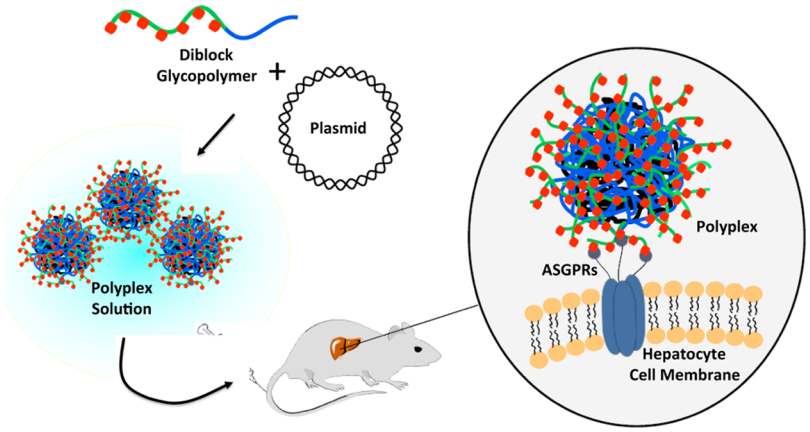

Figure 1. Schematic of polyplex formation and interactions of GalNAc ligands with ASGPRs on hepatocytes. The GalNAc ligands are drawn as red circles, and the cationic blocks are drawn in blue. Cationic blocks complex with plasmids to form polyplexes that display multivalent GalNAc chains on the surface thereby promoting cell type-specific polyplex internalization by binding to ASGPRs.

aggregate with themselves or other biomolecules such as serum proteins, which severely limits the targeting potential of polyplexes to specific tissues when delivered through the circulatory systems of whole animals.[18,21,27] For example, polyplexes formed with PEI become trapped in the lungs during first-pass circulation due to aggregation upon systemic injection.[28,29] Moreover, PEI polyplexes also suffer from rapid clearance from the blood by the reticuloendothelial system due to nonspecific charge-mediated interactions with serum proteins.[30,31] To prevent these detrimental interactions, polyethylene glycol (PEG) is commonly used as a hydrophilic outer layer to sterically stabilize polyplexes from aggregation and prolong circulation times by reducing nonspecific interactions with the reticuloendothelial system.[32,33] However, PEG has a limited effect on polyplex stability and undergoes accelerated blood clearance after multiple injections.[34,35] Several other structures have been explored as alternatives to PEG to achieve colloidal stability and biocompatibility. These include zwitterionic structures like polysulfobetaine, biodegradable polymers such as poly(2-hydroxyethyl methacrylate) and poly(lactic-*co*-glycolic acid).[36−41] Earlier work from our lab has demonstrated that diblock polymers containing glucose or trehalose-substituted monomers copolymerized with a cationic block form colloidally stable polyplexes and offer potential as alternative hydrophilic coating layers.[21,42−45] These sugar-derived neutral blocks form a "stealth" layer that prevents aggregation while maintaining excellent gene-delivery properties in cultured cells.[21,44]

We hypothesized that the highly hydrophilic structure of sugars can serve a dual purpose: maintain colloidal stability of polyplexes and promote tissue-specific delivery by selectively binding to cell surface lectins. To this end, we created a series of cationic diblock glycopolymers derived from *N*-acetyl-D-galactosamine (GalNAc) to target asialoglycoprotein receptors (ASGPRs) on hepatocytes. GalNAc and galactose have been studied extensively for targeting ASGPRs on hepatocytes using mono-, bi-, and triantennary structures to create targeting functionalities.[14,46−53] The triantennary structures have more than a thousand-fold higher affinities to ASGPR compared to monovalent structures based on measured half-maximal inhibitory concentrations (IC_{50}),[50,51] and have facilitated the advancement RNAi therapeutics to clinical trials.[13] However, synthesis of these triantennary structures requires numerous reaction steps that are time, labor, and yield intensive, making it desirable to innovate alternative ligands that can be readily synthesized and applied to a variety of therapeutic cargo.[48,51,54]

Herein, we demonstrate the synthesis of a novel GalNAc-based monomer and its incorporation into diblock polycations exhibiting three cationic block lengths. Complexing the cationic blocks with anionic plasmids (pDNA) aids formation of a core−shell structure that displays the GalNAc blocks on the surface providing a hydrophilic and steric barrier that prevents polyplex aggregation in salt and serum-containing cell culture media, and promotes binding to ASGPRs on hepatocytes (Figure 1). We demonstrate for the first time that this new multivalent GalNAc motif promotes 5 orders of magnitude stronger interactions with ASGPRs than monomeric GalNAc. Preliminary cell culture and mouse biodistribution experiments reveal selective polyplex localization and delivery to the mouse liver. The facile synthesis and assembly of these GalNAc-based block polymers offers a promising new motif to promote both colloidal stability and selective delivery of a wide range of nanomedicine formulations to hepatocytes.

MATERIALS AND METHODS

Materials and Reagents. All the reagents for polymer synthesis were purchased from Aldrich (Milwaukee, WI) at the highest available purity and used as received unless mentioned otherwise. The monomer 2-aminoethylmethacrylamide (AEMA) was purchased from Polysciences (Warrington, PA) and used directly. The chain transfer agent (CTA) 4-cyano-4-(propylsulfanylthiocarbonyl)-sulfanylpentanoic acid (CPP) was synthesized as previously reported.[27,55] The initiator, 4,4′-azobis(4-cyanopentanoic acid) (V-501), was recrystallized twice from methanol prior to use.

All cell culture media used in this study were purchased from Life Technologies (Grand Island, NY): Dulbecco's modified Eagle medium (DMEM, high glucose, Glutamax supplement), reduced-serum medium (Opti-MEM, Glutamax supplement), heat inactivated fetal bovine serum (HI FBS), phosphate-buffered saline (PBS) pH = 7.4, trypsin-EDTA (0.25%), and antibiotic−antimycotic (100×). The MTT reagent (3-(4,5-dimethylthiazol-2-yl)-2,5-diphenyltetrazolium bromide) was purchased from Invitrogen (Carlsbad, CA). Human hepatocellular carcinoma (HepG2, ATCC HB-8065) and human cervical carcinoma (HeLa, ATCC CCL-2) cell lines were purchased from ATCC (Manassas, VA).

gWiz-luc plasmid DNA, used for the luciferase assay, was purchased from Aldevron (Fargo, ND). All other in vitro experiments were performed with pCMV-*lac*Z (Aldevron). Biodistribution experiments in mice were performed with pT2/CAL.[29] Commercially available transfection reagents were used as positive controls in this study.

DOI: 10.1021/acs.biomac.5b01555
Biomacromolecules XXXX, XXX, XXX−XXX

Glycofect (a donation from Techulon, Inc., Blacksburg, VA) and JetPEI (Polyplus-Transfection Inc., Illkirch, France) were used as standards and positive controls for transfections. Unless specified otherwise, all biological experiments were performed in triplicate, and the mean and standard deviation of data are reported in all figures and tables.

Synthesis of the Methacrylamido *N*-Acetyl-D-galactosamine Monomer. *Synthesis of Acetylated GalNAc (**2**).* To a solution of GalNAc (**1**; 5.15 g, 23.9 mmol) in dry pyridine (240 mL) at room temperature was added acetic anhydride (20.0 g, 196 mmol), DMAP (0.0280 g, 0.238 mmol), and stirred for 12 h. After 12 h, the reaction mixture was diluted with ethyl acetate (240 mL), and washed with 1 N HCl solution (3 × 100 mL). The organic layer was then washed with satd $NaHCO_3$ (1 × 100 mL), distilled water (1 × 100 mL), and brine (1 × 100 mL), dried with Na_2SO_4, and filtered. The solvent was concentrated under reduced pressure and dried under high vacuum to afford 7.20 g (18.8 mmol, 78% yield) of acetylated GalNAc (**2**) as white foam. IR (film) 3286, 1741, 1677, 1657, 1558, 1540, 1369, 1321, 1211, 1108, 1009, 937; ^{1}H NMR (300 MHz) δ 6.21 (d, J = 6.0 Hz, 1H), 5.43 (m, 2H), 5.22 (dd, J = 15.0, 3 Hz, 1H), 4.73 (m, 1H), 4.24 (m, 1H), 4.1 (m, 2H), 2.17 (bs, 6H), 2.03 (bs, 6H), 1.95 (s, 3H); ^{13}C NMR (125 MHz) δ 171.09, 170.39, 170.35, 170.22, 168.91, 91.24, 68.49, 67.74, 66.68, 61.29, 46.94, 23.07, 20.94, 20.73, 20.64, 20.62; HRMS (ESI) Calcd for $C_{16}H_{23}NO_{10}$ + Na, 412.1220; found, 412.1214.

*Synthesis of 1,2-Oxazoline (**3**).* To a solution of **2** (4.87 g, 12.5 mmol) in 1,2-dichloroethane (130 mL) under a nitrogen atmosphere was added trimethylsilyl trifluoromethanesulfonate (TMSOTf) (3.06 g, 13.8 mmol), and the solution was heated to 50 °C and stirred for 12 h. After, it was cooled down to room temperature, triethylamine was added to neutralize the solution. Post-neutralization, the solution was concentrated under reduced pressure, and the crude mixture was dried under vacuum. The product was purified via column chromatography by eluting the product in a 20:1 $CHCl_3$/MeOH mobile phase. Semipure oxazoline (**3**, 4.00 g) was isolated from the column and taken directly to the next step.

*Synthesis of Acetylated MAGalNAc (**5**).* To a solution of **3** (4.00 g) in 1,2-dichloroethane (72 mL) under a nitrogen atmosphere was added 2-hydroxyethylmethacrylamide (**4**; 5.55 g, 43 mmol) and camphor sulfonic acid (CSA, 0.333 g, 1.43 mmol) and refluxed for 12 h. After, the solution was cooled to room temperature and neutralized with triethylamine. The crude was then concentrated under reduced pressure and dried under high vacuum. The product was then purified via column chromatography where it was eluted with a 20:1 $CHCl_3$/MeOH mobile phase. IR (film) 3293, 3078, 2935, 1744, 1658, 1619, 1533, 1433, 1369, 1304, 1221, 1166, 1135, 1074, 1044, 929, 733, 589 cm^{-1}; ^{1}H NMR (500 MHz) δ 6.44 (m, 1H), 5.89 (m, 1H), 5.76 (s, 1H), 5.35 (s, 1H), 5.35 (m, 1H), 5.11 (dd, J = 15, 5 Hz, 1H), 4.62 (d, J = 5 Hz, 1H), 4.14 (m, 3H), 3.91 (m, 2H), 3.71 (m, 2H), 3.39 (m, 1H), 2.15 (s, 3H), 2.05−1.94 (m, 12H); ^{13}C NMR (125 MHz) δ 171.11, 170.65, 170.46, 170.21, 168.81, 139.65, 120.2, 100.97, 70.83, 70.30, 68.04, 66.57, 61.48, 51.05, 39.12, 23.26, 20.70 (3C), 18.65; HRMS (ESI) Calcd for $C_{20}H_{30}N_2O_{10}$ + Na, 481.1798; found, 481.1806.

*Synthesis of MAGalNAc (**6**).* To a solution of **5** (3.60 g, 8.10 mmol) in MeOH (300 mL), sodium methoxide (2.72 g, 33.2 mmol) was added to obtain a solution pH of ∼9. The reaction was stirred for 12 h, and then the solution was neutralized with Dowex 50W×2 hydrogen form resin. The resin was filtered and the solution was concentrated under reduced pressure and dried under vacuum. The product was then redissolved in water and lyophilized to dryness. No further purification was required. IR (film) 3306, 2926, 1651, 1613, 1529, 1433, 1372, 1310, 1206, 1156, 1115, 1051, 930, 584 cm^{-1}; ^{1}H NMR (500 MHz) δ 5.62 (s, 1H), 5.38 (s, 1H), 4.36 (d, J = 10 Hz, 1H), 3.9−3.5 (m, 8H), 3.45−3.27 (m, 2H), 1.9 (s, 3H), 1.84 (s, 3H); ^{13}C NMR (125 MHz) δ 174.66, 171.80, 138.89, 121.23, 101.48, 75.05, 70.96, 67.85, 67.72, 60.93, 52.34, 39.36, 22.15, 17.61; HRMS (ESI) Calcd for $C_{14}H_{24}N_2O_7$ + Na, 355.1481; found, 355.1484.

Synthesis and Characterization of MAGalNAc Polymers. *Synthesis of PMAGalNAc$_{62}$ by RAFT Polymerization.* A solution of CPP (0.00900 g, 0.0320 mmol), MAGalNAc (0.765 g, 2.3 mmol), and V-501 (8.80 × 10^{-4} g, 0.00320 mmol) in 4.6 mL of 4:1 H_2O/methanol was added to a 25 mL round-bottom flask equipped with a magnetic stir bar. The stirred solution was then sparged with nitrogen for 30 min, and the flask was placed in a preheated oil bath at 70 °C. The reaction was terminated after 6 h by quenching the reaction flask in liquid nitrogen, followed by exposure to air. After purification by dialysis against water (pH 4−5) and lyophilization, the PMAGalNAc$_{62}$ macroCTA was chain extended with AEMA to yield three diblock polymers following a similar procedure, as previously published.[45] In general, AEMA (0.132 g, 0.799 mmol), PMAGalNAc$_{62}$ (0.100 g), and V-501 (2.60 × 10^{-4} g, 9.40 × 10^{-4} mmol) were dissolved in 7.9 mL of 1 M acetate buffer (pH 5.2) and added to a 25 mL round-bottom flask equipped with a magnetic stir bar. After sparging with nitrogen for 30 min, the stirred reaction was allowed to proceed at 70 °C for 7.5 h. The reaction mixture was then quenched by cooling the reaction vessel in liquid nitrogen and exposing to air. The product was purified by dialysis against DI water (pH adjusted to between 4 and 5 by addition of HCl) and lyophilized to dryness.

Size exclusion chromatography (SEC) was used to determine the molecular weight (number-average, M_n and weight-average, M_w) and dispersity ($Đ$) for the PMAGalNAc$_{62}$ macroCTA and the block copolymers of MAGalNAc and AEMA using an aqueous eluent of 1.0 wt % acetic acid/0.1 M Na_2SO_4. A flow rate of 0.4 mL/min, Eprogen (Downers Grove, IL) columns [CATSEC1000 (7 μm, 50 × 4.6), CATSEC100 (5 μm, 250 × 4.6), CATSEC300 (5 μm, 250 × 4.6), and CATSEC1000 (7 μm, 250 × 4.6)], a Wyatt HELEOS II light scattering detector (λ = 662 nm), and an Optilab rEX refractometer (λ = 658 nm) were used. Astra V (version 5.3.4.18, Wyatt Technologies, CA) was utilized for the determination of M_n, $Đ$, and dn/dc of the (co)polymers. ^{1}H NMR measurements were performed with a temperature-controlled Varian 400-MR (Palo Alto, CA) spectrometer operating at a frequency of 399.7 MHz in D_2O (HOD internal standard). Block polymer compositions were determined by comparing resonances of the MAGalNAc block with those associated with the AEMA block.

Polyplex Formulation and DNA Binding Studies by Gel Electrophoresis. All polyplex solutions were prepared in DNase/RNase-free water, unless otherwise specified. Stock solutions of polymer were prepared in water at a concentration of 15 mM ionizable amines. The stock solutions were diluted in water to appropriate concentrations necessary for the desired N/P ratios. Polyplexes were formulated by adding an equal volume of polymer solution to pDNA in water. For DNA-binding studies by gel electrophoresis, aqueous polymer solutions (10 μL) at appropriate concentrations were added to 10 μL of pDNA solution (50 ng/μL) to make polyplexes at various N/P values. For example, to achieve N/P = 5, the stock polymer solution was diluted to 0.75 mM of ionizable amines before adding 10 μL of it to pDNA solution at 50 ng/μL (0.15 mM phosphates). Polyplex formulations were kept at room temperature to equilibrate for 1 h before running them on a 0.6% agarose gel containing 0.3 μg/mL ethidium bromide. Gel electrophoresis was carried out at 80 V for 45 min. The binding of pDNA to cationic polymers resulted in its retardation on the gel which was visualized and imaged (Figure S10) with a Fotodyne FOTO/Analyst Luminary/FX workstation from Fotodyne (Hartland,WI).

Particle Size and Zeta Potential Measurements. The particle size and zeta potential measurements were carried out by dynamic light scattering using Zetasizer Nano-ZS from Malvern Instruments Ltd. (Malvern, U.K.) For particle size measurements, polypexes were prepared by adding 25 μL of aqueous polymer solutions to 25 μL of pDNA (20 ng/μL in water). The polymer concentrations were adjusted to achieve N/P ratios of 2.5, 5, and 7.5, as described earlier. The mixture was incubated for an hour before adding 100 μL of Opti-MEM. The sample was analyzed immediately to determine the particle size at 0 h. Additional measurements were performed after 2 and 4 h to study the stability of polyplexes over time. Z-average diameters calculated by the instrument at 0, 2, and 4 h time points are reported. For zeta potential measurements, 150 μL of aqueous polymer solution was added to 150 μL pDNA (20 ng/μL in water) to achieve N/P values of 2.5 and 5. After equilibration at room temperature for an

DOI: 10.1021/acs.biomac.5b01555
Biomacromolecules XXXX, XXX, XXX−XXX

hour, 600 μL of water was added to each sample. The zeta potential was measured at a detection angle of 17°.

Cell Culture. HepG2 and HeLa cells were cultured in DMEM containing 10% FBS in 75 cm^2 flasks at 37 °C under 5% CO_2 atmosphere to maintain physiological pH. The culture medium was supplemented with Antibiotic−Antimycotic solution from Life Technologies (Grand Island, NY) at a final concentration of 10 μg/mL penicillin, 10 μg/mL streptomycin, and 25 ng/mL Fungizone. Cells were monitored for confluency regularly and passaged as necessary. For plating, cells were trypsinized and suspended in DMEM containing 10% FBS. A hemocytometer was used to count cells prior to plating. Trypan blue was used to distinguish between viable and dead cells. For MTT and luciferase assays, 50000 viable cells in 1 mL of DMEM containing 10% FBS were plated per well in 24-well plates.

Cell Viability Assay. Polyplexes were prepared an hour before transfection by adding 175 μL of aqueous polymer solutions at appropriate concentrations to 175 μL of pDNA (20 ng/μL in water) to achieve desired N/P values (2.5, 5, and 7.5), as described earlier. Prior to transfection, the polymer−pDNA mixtures were vortexed and incubated at room temperature for an hour. Transfections were carried out 24 h after plating. The medium was aspirated from each well and then cells were washed once with 1× PBS. Polyplexes were diluted 2-fold with Opti-MEM. The diluted solution (300 μL) was then added to each well. Four hours after incubation at 37 °C and 5% CO_2, 1 mL of DMEM containing 10% FBS was added to each well. At 24 h post-transfection, the media was replaced with 1 mL of DMEM containing 10% FBS and 0.5 mg/mL MTT. Cells were incubated at 37 °C and 5% CO_2 for an hour and then the medium was aspirated from each well. The cells were then washed once with 1× PBS, and 600 μL of DMSO was added to each well to lyse the cells. The plates were placed on an orbital shaker for 15 min to allow complete cell lysis. An aliquot (200 μL) was removed from each well and transferred to a clear 96-well plate. Absorbance was measured at 570 nm using a TECAN GENios Pro microplate reader from Tecan (Männedorf, Switzerland). Data were normalized such that the negative control (cells that were not transfected) had a cell viability of 100%.

Competitive Inhibition of Cy5-Labeled Asialofetuin. Asialofetuin, a known ligand of ASGPRs, was purchased from Aldrich (Milwaukee, WI). Cy5-NHS ester from Cyandye (Sunny Isles Beach, FL) was dissolved in PBS containing 50% DMSO creating a stock solution of 2.5 mM. The Cy5 labeling reaction contained 0.1 mM ASF and 0.5 mM Cy5-NHS in a total volume of 1.1 mL. The mixture was kept on ice for 10 h to allow the reaction to proceed. After 10 h, protein was purified from the mixture using Amicon Ultra-0.5 centrifugal filters (30 kDa nominal molecular weight limit) by buffer exchange with Imject purification buffer from Life Technologies (Grand Island, NY). The buffer exchange was performed to achieve a million-fold dilution of the original buffer. The final volume (1 mL) of purified ASF-Cy5 was aliquoted into 100 μL fractions, flash frozen in liquid nitrogen, and stored at −80 °C until further use. The protein concentration and Cy5 labeling efficiency were determined by UV−vis using a NanoDrop 2000c instrument from NanoDrop Products (Wilmington, DE). The labeling reaction achieved approximately 1.7 Cy5 labels per molecule of ASF, as determined by UV−vis. For competitive inhibition studies, HepG2 cells were cultured and trypsinized, as described earlier. Cells were washed once with DMEM containing 10% FBS to deactivate and remove trypsin/EDTA. The inhibition experiments were carried out in a volume of 1 mL of DMEM containing 10% FBS, 6 nM ASF-Cy5, and various concentrations of inhibitors prepared by serial dilutions. Each sample contained 200000 cells, which were incubated at 37 °C for 2 h in 5% CO_2 environment prior to analysis. Cells were washed twice with PBS before running them on a BD FACSVerse from BD Biosciences (San Jose, CA). Measurements were performed in triplicate, and the median Cy5 intensity of each cell population was used in data analysis. The median intensity of samples containing no inhibitor was normalized to 100 and the uptake of ASF-Cy5 in all other samples was reported as a percentage of that value in Figure 4. The IC_{50} values were estimated by fitting data to the Hill equation.[56]

Luciferase Assay. For luciferase gene expression assays, HepG2 or HeLa cells were transfected in 24-well plates at a density of 50000 cells/well in 1 mL of DMEM containing 10% FBS. Polyplexes were prepared an hour before transfection by adding 175 μL of aqueous polymer solutions at appropriate concentrations to 175 μL of pDNA (20 ng/μL in water) to achieve desired N/P values (2.5 and 5), as described earlier. The polymer−pDNA mixtures were vortexed and kept at room temperature for an hour. Transfections were carried out 24 h after plating. DMEM was aspirated off from each well and cells were washed with 1× PBS. Polyplexes were diluted two times with either reduced-serum Opti-MEM or DMEM containing 10% FBS. The diluted solution (300 μL) was then added to each well. Four hours after transfection, 1 mL of DMEM containing 10% FBS was added to each well. A total of 24 h after transfection, culture medium was replaced with fresh DMEM containing 10% FBS. A total of 48 h after transfection, the culture medium was aspirated off and the cells were washed with 1× PBS. The luciferase assay system was purchased from Promega (Madison, WI). An aliquot (100 μL) of 1× lysis buffer was added to each well and kept at room temperature for a minimum of 10 min to allow cell lysis to occur. Cell lysate (5 μL) was then pipetted into an opaque white 96-well plate. After addition of 100 μL of luciferase substrate, the luminescence was measured using a TECAN GENios Pro microplate reader (Tecan, Männedorf, Switzerland). Protein concentration in each sample was measured using Quick Start Protein Assay Kit from Bio-Rad Laboratories (Hercules, CA).

Biodistribution Studies in Mice. All animal work was carried out in accordance with IACUC guidelines. Animals were housed in the Research Animal Resources facility at the University of Minnesota. For in vivo biodistribution studies, a 40 μg dose of pDNA was delivered with polymers P(MAGalNAc$_{62}$-*b*-AEMA$_{33}$), P(MAG$_{46}$-*b*-AEMA$_{13}$), or in vivo-jetPEI via tail-vein injections in C57BL/6J mice. Three mice were injected for each study group, unless otherwise stated. Polyplexes were formulated in a 5% dextrose solution. At day 1, mice were given intraperitoneal injections of 100 μL of 25 mg/mL D-luciferin and imaged with an IVIS Spectrum Preclinical In Vivo Imaging System from PerkinElmer Inc. (Waltham, MA). Animals were euthanized immediately using carbon dioxide, and tissues (liver, left lung, heart, left kidney, spleen) and blood were collected. All the samples were flash-frozen in liquid nitrogen and stored at −80 °C until further processing. DNA was purified from the tissues by phenol−chloroform extraction. The amount of plasmid DNA in each tissue was determined by quantitative polymerase chain reaction (qPCR), run by the University of Minnesota Genomics Center using primers 5′-tgagtact-tcgaaatgtccgttc-3′ and 5′-gtattcagcccatatcgtttcat-3′. The data are presented as fold difference from background (tissues from wild-type C57BL/6J mouse) of pDNA per genome equivalent of total DNA.

To quantify the amount of polymer in various tissues, P(MAGalNAc$_{62}$-*b*-AEMA$_{33}$) and P(MAG$_{46}$-*b*-AEMA$_{13}$) were labeled with a Cy7 fluorophore using Cy7-NHS ester from Lumiprobe (Hallandale Beach, FL) according to manufacturer's protocol. The extent of labeling was calculated based on the absorbance due to Cy7 at 747 nm. Approximately 2% of the amines in both the polymer samples were found to carry the Cy7 label. Dynamic light scattering of labeled polymer−DNA complexes showed no significant change from unlabeled samples (data not shown). Three mice each were injected with 40 μg of pT2/CAL complexed with the Cy7-labeled polymers at desired N/P ratios. Mice were euthanized 30 min after injections, and the tissues (liver, left lung, heart, left kidney, spleen) and blood were harvested. All the samples were stored at −80 °C. Tissues were imaged for Cy7 content with the IVIS Spectrum Preclinical In Vivo Imaging System from PerkinElmer Inc. (Waltham, MA). The background fluorescence was subtracted from each sample. The distribution data for individual tissues are presented as a fraction of total fluorescence in all the harvested samples.

RESULTS AND DISCUSSION

Synthesis and Characterization of Diblock Glycopolymers. To create the targeted delivery vehicles, two methacrylamide-based monomers were selected for controlled

DOI: 10.1021/acs.biomac.5b01555
Biomacromolecules XXXX, XXX, XXX−XXX

Scheme 1. Synthesis of Methacrylamido *N*-Acetyl-D-galactosamine[a]

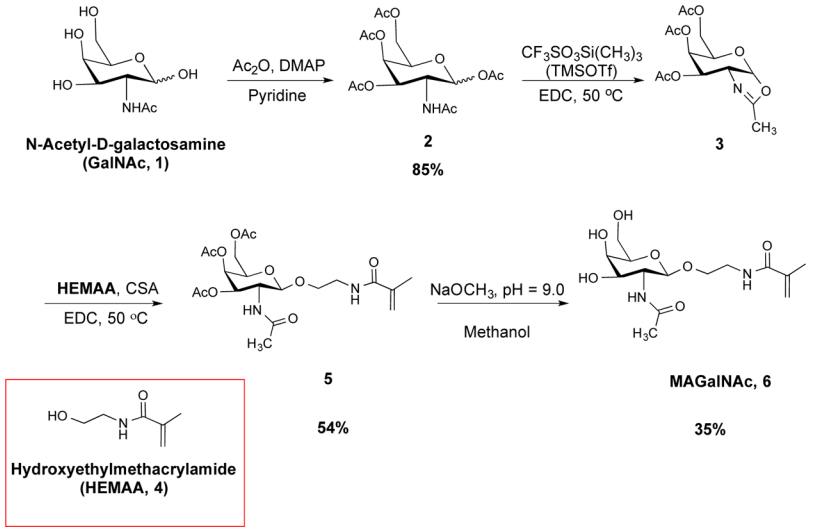

[a]Reagents and conditions: (Step 1) Acetic anhydride (Ac_2O), 4-dimethylaminopyridine (DMAP), pyridine (yield = 85%). (Step 2) Trimethylsilyl trifluoromethanesulfonate (TMSOTf), ethylene dichloride (EDC), 50 °C. (Step 3) *N*-Hydroxyethyl acrylamide (HEMAA; structure shown in the red box), camphorsulfonic acid (CSA), EDC, 90 °C (overall yield = 54%). (Step 4) Sodium methoxide ($NaOCH_3$), pH = 9.0, methanol (overall yield = 35%).

Scheme 2. Synthesis of GalNAc-Based Diblock Polymers[a]

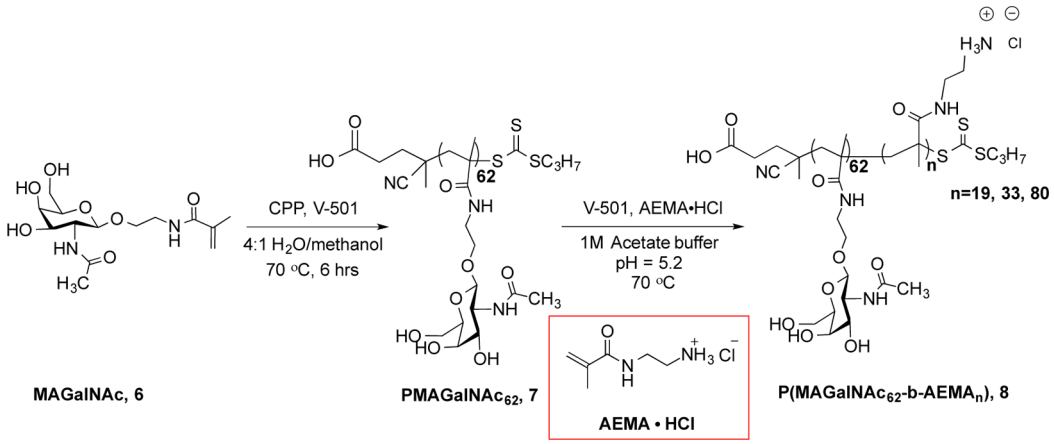

[a]Reagents and conditions: (Step 1) 4-Cyano-4-(propylsulfanylthiocarbonyl) sulfanylpentanoic acid (CPP), 4,4′-azobis(4-cyanopentanoic acid) (also known as V-501), 4:1 H_2O/methanol mixture, 70 °C. (Step 2) V-501, 2-aminoethylmethacrylamide hydrochloride (AEMA·HCl) (structure shown in the red box), 1 M acetate buffer (pH = 5.2), 70 °C.

polymerization by the Reversible Addition−Fragmentation Chain Transfer (RAFT) mechanism.[57] The first monomer, 2-aminoethylmethacrylamide (AEMA), was selected to create the polycation block to facilitate binding to pDNA, and a second monomer based on GalNAc was designed to create the ASGPR-targeting functionality. The GalNAc-derived monomer, methacrylamido *N*-acetyl-D-galactosamine (denoted as MAGalNAc, **6**), was synthesized in four steps, as shown in Scheme 1. The hydroxyl groups of *N*-acetyl-D-galactosamine (GalNAc, **1**) were first acetylated to create *O*-acetyl GalNAc (**2**). The acetylated product **2** was then treated with trimethylsilyl trifluoromethanesulfonate (TMSOTf) in dichloroethane at 50 °C to yield 1,2-oxazoline (**3**).[58] The oxazoline was ring-opened with hydroxyethylmethacrylamide (HEMAA, **4**) to synthesize *O*-acetyl MAGalNAc (**5**). Lastly, the *O*-acetyl groups of **5** were cleaved by methanolysis at pH = 9 to yield the final methacrylamido-monomer structure, MAGalNAc (**6**).

A trithiocarbonate chain transfer agent (CTA), 4-cyano-4-(propylsulfanylthiocarbonyl) sulfanylpentanoic acid (CPP) was used to achieve control over radical polymerization. The initial RAFT studies on MAGalNAc (**6**) were performed on a 100−200 mg scale, which lead to approximately 60% conversion in 6 h with low dispersity values ($Đ$ < 1.1). To produce a large batch of polymer to carry through for numerous analytical and biological characterizations, 1 g of MAGalNAc (**6**) was polymerized in the presence of CPP and a free radical initiator 4,4′-azobis(4-cyanopentanoic acid) in a 4:1 H_2O/MeOH mixture at 70 °C for 6 h. As shown in Scheme 2, the macroCTA poly(methacrylamido *N*-acetyl-D-galactosamine) or $PMAGalNAc_{62}$ was synthesized in high yield (92%) and low dispersity ($Đ$ = 1.17) at this larger scale. This macroCTA was isolated by dialysis against water using a 3.5 kDa MWCO dialysis bag. The $PMAGalNAc_{62}$ macroCTA was subsequently chain-extended with AEMA to produce three diblock polymers

DOI: 10.1021/acs.biomac.5b01555
Biomacromolecules XXXX, XXX, XXX−XXX

with AEMA repeat units of 19, 33, and 80 (Table 1). AEMA polymerizations were performed in 1 M aqueous acetate buffer (pH = 5.2) to minimize hydrolysis and maintain the trithiocarbonate chain end groups.

Table 1. Molecular Weight, Dispersity, and Degree of Polymerization (DP) of Polymers

polymer	M_n[a]	$Đ$[a]	MAGalNAc DP[a]	AEMA DP[a]
$PMAGalNAc_{62}$	20	1.17	62	N/A
$P(MAGalNAc_{62}$-*b*-$AEMA_{19})$	23	1.29	62	19
$P(MAGalNAc_{62}$-*b*-$AEMA_{33})$	25	1.32	62	33
$P(MAGalNAc_{62}$-*b*-$AEMA_{80})$	31	1.32	62	80
$P(EG_{45}$-*b*-$AEMA_{32})$	6.5	1.11	N/A	32
$P(MAG_{46}$-*b*-$AEMA_{13})$[b]	13.1	1.02	N/A	13

[a]Number-average molecular weight (M_n) in kilodaltons (kDa) and dispersity ($Đ$), as determined by SEC using an aqueous eluent of 0.1 M Na_2SO_4 in 1 wt % acetic acid at a flow rate of 0.3 mL/min on Eprogen columns [CATSEC1000 (7 μm, 50 × 4.6), CATSEC100 (5 μm, 250 × 4.6), CATSEC300 (5 μm, 250 × 4.6), and CATSEC1000 (7 μm, 250 × 4.6)] with a Wyatt HELEOS II static light scattering detector (λ = 662 nm) and an Optilab rEX refractometer (λ = 658 nm). [b]The synthesis and characterization of $P(MAG_{46}$-*b*-$AEMA_{13})$ has been reported previously.[45]

As a control, a PEG-based block polycation was also prepared by extending a PEG macroCTA (M_n = 2400, 45 repeat units of ethylene glycol) with AEMA (Scheme 3) to create $P(EG_{45}$-*b*-$AEMA_{32})$. A previously published glucose-derived block polycation, $P(MAG_{46}$-*b*-$AEMA_{13})$, containing poly(methacrylamido glucopyranose) neutral block was used as an additional control.[45] These controls were studied to examine the specificity of sugar blocks in hepatocyte-targeted delivery.

MAGalNAc and PEG block polycations were analyzed by size-exclusion chromatography (SEC) to measure dispersities and number-average molecular weights (Table 1). SEC chromatograms of $PMAGalNAc_{62}$ and the diblock polymers were unimodal with moderate dispersities ($Đ$ < 1.35). The moderate dispersities of the diblock polymers may be attributed to the monomer-starved conditions accompanying the high percent conversion (92%) during the synthesis of $PMAGalNAc_{62}$ macroCTA. The number-average molecular weights were used to calculate degree of polymerizations. Block polymer compositions were confirmed by comparing ^1H NMR resonances of the MAGalNAc block with those associated with the AEMA block.

Polyplex Formulation and Size Measurements. To examine the interactions of pDNA with each of the block copolycations, polymer solutions were added to pDNA solutions (50 ng/μL), vortexed, and kept at room temperature for 1 h. The N/P ratio of each polyplex formulation was calculated as the molar ratio of ionizable amines on the polymer ("cationic block") to phosphates on the pDNA. In the polymerized form, the average pK_a of the AEMA amine groups is 8.5.[44] As a result, 93% of the amines are expected to be in the protonated form when the polyplexes are formulated in water and added to cell culture media (pH = 7.4). Polyplex formation was confirmed by the lack of pDNA migration through agarose gels (Figure S10). $P(MAGalNAc_{62}$-*b*-$AEMA_{19})$ and $P(EG_{45}$-*b*-$AEMA_{32})$ significantly retarded the migration of pDNA at N/P values of 2 and above. $P(MAGalNAc_{62}$-*b*-$AEMA_{33})$ and $P(MAGalNAc_{62}$-*b*-$AEMA_{80})$ achieved the same effect at N/P values above 2.5. Based on these results, N/P values of 2.5, 5, and 7.5 were selected to evaluate polyplex stability and cytotoxicity.

Polyplex sizes were measured by dynamic light scattering to study the colloidal stability in biological media over time (Figure 2). The hydrodynamic diameters of polyplexes at N/P ratios of 2.5, 5, and 7.5 ranged from 90 to 160 nm when measured immediately after dilution with reduced-serum Opti-MEM. The polyplexes formed with $P(MAGalNAc_{62}$-*b*-$AEMA_{19})$ and $P(MAGalNAc_{62}$-*b*-$AEMA_{33})$ were found to be more colloidally stable in reduced-serum Opti-MEM compared to $P(EG_{45}$-*b*-$AEMA_{32})$ polyplexes. After 4 h at room temperature, $P(MAGalNAc_{62}$-*b*-$AEMA_{19})$ and $P(MAGalNAc_{62}$-*b*-$AEMA_{33})$ polyplexes formulated at N/P of 2.5 and 5 showed no statistically significant increase in diameter. Similarly, $P(MAG_{46}$-$AEMA_{13})$ polyplexes at N/P of 5 were previously shown to maintain their size at approximately 100 nm over 4 h.[45] In contrast, $P(EG_{45}$-*b*-$AEMA_{32})$ polyplexes exhibited an increase of 140 and 56 nm during the same time period at N/P ratios 2.5 and 5, respectively, which could be attributed to the less bulky nature of the PEG_{45} block conferring less effective steric stabilization. $P(MAGalNAc_{62}$-*b*-$AEMA_{80})$ polyplexes were found to aggregate to a higher extent than polyplexes formed with shorter cationic blocks. This difference is likely the result of fewer polymer chains (and, thus, fewer hydrophilic sugar blocks) present at the same N/P values with this polymer compared to the shorter cationic block polymers. The presence of fewer MAGalNAc blocks coating the polyplexes imparts lower steric hindrance, and thus less protection from aggregation. This highlights the role of the neutral/hydrophilic sugar blocks in promoting polyplex colloidal stability.

Scheme 3. Synthesis of PEG-Based Cationic Polymer $P(EG_{45}$-*b*-$AEMA_{32})$[a]

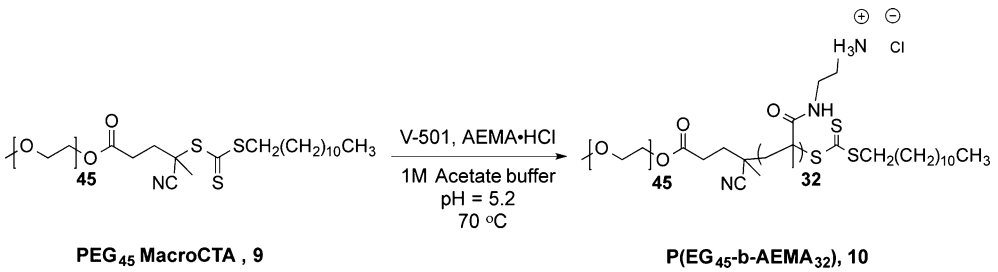

PEG_{45} MacroCTA , 9 — $P(EG_{45}$-b-$AEMA_{32})$, 10

[a]Reagents and conditions: 4,4′-azobis(4-cyanopentanoic acid) (also known as V-501), 2-aminoethylmethacrylamide hydrochloride (AEMA·HCl), 1 M acetate buffer (pH = 5.2), 70 °C.

DOI: 10.1021/acs.biomac.5b01555
Biomacromolecules XXXX, XXX, XXX−XXX

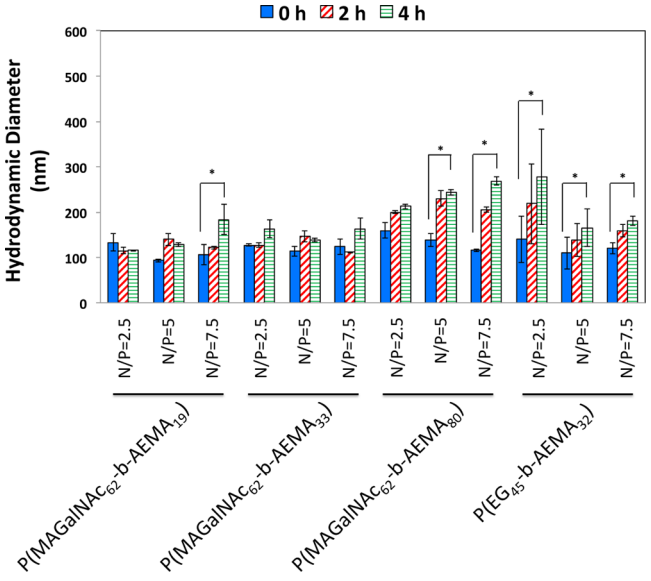

Figure 2. Hydrodynamic diameters of polyplexes as measured by dynamic light scattering. Polyplexes were formed by mixing equal volumes of pDNA and polymer solutions at N/P ratios of 2.5, 5, and 7.5. The mixtures were incubated at room temperature for 1 h before adding twice the volume of reduced-serum Opti-MEM. The time of Opti-MEM addition is indicated as 0 h, with additional measurements reported at 2 and 4 h as mean ± standard deviation (n = 3). Data were analyzed by paired t test. The asterisks (*) indicate that the measurements were statistically different (p < 0.05).

Cell Viability Studies. The viability of HepG2 cells (Figure 3), derived from human hepatocellular carcinoma, and HeLa

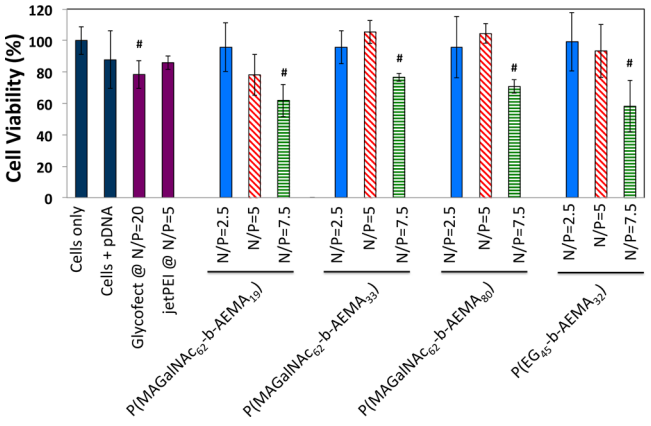

Figure 3. HepG2 cell viability as measured by MTT assay. Cells were transfected with polyplexes formed at N/P ratios of 2.5, 5, and 7.5 in Opti-MEM. At 24 h post-transfection, cells were incubated with DMEM containing 10% FBS and 0.5 mg/mL MTT for 15 min, washed with PBS, and lysed by the addition of DMSO. Data were normalized to indicate 100% cell viability for the untransfected control (cells only) and reported as mean ± standard deviation (n = 3). A number sign (#) is used to mark measurements that were statistically different (p < 0.05) from the cells only control.

cells (Figure S12), derived from human cervical adenocarcinoma, following treatment with the polyplex formulations in Opti-MEM was assessed by MTT (3-(4,5-dimethylthiazol-2-yl)-2,5-diphenyltetrazolium bromide) assay. In general, treatment with PMAGalNAc and PEG polyplexes resulted in lower HepG2 cell viability at higher N/P ratios. At N/P ratios of 2.5 and 5, the PMAGalNAc and PEG-based block polymers showed similar cell viabilities compared to untransfected controls; however, a statistically significant decrease in viability was observed at a N/P ratio of 7.5. In contrast, earlier work has shown no cytotoxicity up to a N/P ratio of 10 with P(MAG_{46}-b-$AEMA_{13}$) polyplexes. Based on these results and the size measurements discussed earlier, subsequent gene delivery studies were carried out at N/P ratios of 2.5 and 5.

Competitive Inhibition of ASGPR-Mediated Uptake. We hypothesized that incorporation of GalNAc ligands into a polymeric chain would facilitate multivalent interactions with the carbohydrate recognition domains of ASGPRs leading to enhanced binding affinity and internalization in hepatocytes. To test this hypothesis, the ability of GalNAc-derived glycopolymers to inhibit internalization of asialofetuin (ASF) by a hepatocyte cell line (HepG2) was examined. Asialofetuin is known to contain bi- and triantennary ligands that facilitate cellular binding and ASGPR-mediated uptake.[59−62] Competitive inhibition experiments were performed in suspended HepG2 cells to estimate relative binding affinities of various ligands including $PMAGalNAc_{62}$, ASF, GalNAc, galactose, $PMAG_{62}$, and glucose as inhibitors. Cells were incubated with 6 nM Cy5-labeled ASF (ASF-Cy5) in DMEM containing 10% FBS for 2 h at 37 °C in the presence of various concentrations of the inhibitors. Figure 4 shows the uptake profile of ASF-Cy5 into HepG2 cells, as measured by flow cytometry. $PMAGalNAc_{62}$ effectively inhibited the uptake of Cy5-labeled asialofetuin at considerably lower concentrations (half-maximal

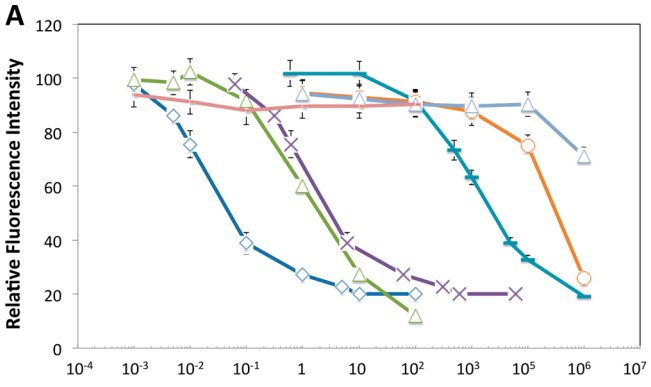

B

Symbol	Inhibitor	IC_{50} (μM)
	$PMAGalNAc_{62}$	0.02±0.005
	ASF	1±0.3
	62*$PMAGalNAc_{62}$	1±0.3
	GalNAc	1000±100
	Galactose	N.D.
	Glucose	N.D.
	$PMAG_{62}$	N.D.

Figure 4. (A) Competitive inhibition of Cy5-labeled asialofetuin (ASF-Cy5) uptake by HepG2 cells in the presence of various compounds: $PMAGalNAc_{62}$ (blue diamonds), ASF (green triangles), 62*$PMAGalNAc_{62}$ ($PMAGalNAc_{62}$ concentration expressed in GalNAc equivalents; purple crosses), GalNAc (blue dashes), galactose (orange circles), and glucose (light blue triangles), and $PMAG_{62}$ (pink dashes). Data are reported as mean ± standard deviation (n = 3). (B) IC_{50} values estimated by fitting data to the Hill equation. N.D. = not determined.

DOI: 10.1021/acs.biomac.5b01555
Biomacromolecules XXXX, XXX, XXX−XXX

inhibitory concentration, IC_{50} = 20 nM) than monomeric GalNAc (IC_{50} = 1 mM) and asialofetuin (IC_{50} = 1 μM). Consistent with earlier reports, IC_{50} values followed the order ASF < GalNAc < galactose < glucose.[60,63,64] To further highlight the strong affinity of $PMAGalNAc_{62}$, we plotted these data using a "GalNAc equivalent" concentration (i.e., concentration of $PMAGalNAc_{62}$ polymer chains multiplied by 62, denoted as 62*$PMAGalNAc_{62}$ in Figure 4). The inhibition by one GalNAc unit in the polymer was comparable to ASF and much greater than free GalNAc when compared with the GalNAc equivalent concentration of $PMAGalNAc_{62}$ chains. These data suggest that multivalent binding imparts higher receptor affinity, in accordance with previous findings on the effect of ligand valency on binding affinity to ASGPRs.[50,51,65,66] Previous studies have used ligand-functionalized, radiolabeled proteins at 4 °C for measuring IC_{50} values to show that biantennary and triantennary structures can have 3−4 orders of magnitude higher binding constants compared to monovalent structures.[50,54] Uptake studies of fluorescently labeled compounds at 37 °C (similar to our current study) have also shown a similar trend[51,66] with biantennary and triantennary ligands, even though the IC_{50} values differ between these two approaches due to differences in experimental design. These data suggest that a serial arrangement of GalNAc in a block of 62 repeat units also provides high binding affinity due to the cluster glycoside effect (yielding 5 orders of magnitude higher affinity than free GalNAc).[67] This work is the first report of using polymerized GalNAc ligands to achieve high ligand−receptor affinity and provides a facile alternative to the labor-intensive synthesis of bi- or triantennary structures currently used for ASGPR targeting.

Transgene Expression in Transfected Cultured Cells. Transfection efficiency was studied by quantifying expression of a luciferase reporter gene from each polyplex formulation in cell culture. HepG2 and HeLa cells were transfected with polyplexes containing gWiz-luc plasmid (sourced from Aldevron, Fargo, ND) at N/P ratios of 2.5 and 5. We hypothesized that ASGPR receptors on HepG2 cells will facilitate uptake of plasmids complexed with the cationic block polymers containing polymerized GalNAc ligands. In agreement with our hypothesis, HepG2 cells exhibited higher luciferase activity than HeLa cells when gWiz-luc was delivered with GalNAc-derived block polymers (Figure 5). HepG2 cells display approximately 76000 ASGPRs per cell that can bind with the ligands in MAGalNAc polyplex formulations.[68] The lack of these receptors on HeLa cells leads to lower gene uptake, and therefore a lower transgene expression compared to HepG2 cells. In contrast to MAGalNAc-containing formulations, the $P(MAG_{46}$-*b*-$AEMA_{13})$, $P(EG_{45}$-*b*-$AEMA_{32})$, and JetPEI controls showed similar or higher gene expression in HeLa compared to HepG2 cells. Interestingly, efficient gene delivery is achieved at low N/P ratios (2.5 and 5) compared to previously reported nontargeted glycopolycations that required N/P ratios up to 20.[21,43,45,69] These data suggest that the positive charge or excess free polymer may play a more important role in nonspecific cell surface interactions and uptake of nontargeted systems compared to the receptor-mediated uptake mechanism promoted by targeting ligands.[70,71] When polyplexes were formulated with a mixture of $P(MAGalNAc_{62}$-*b*-$AEMA_{33})$ and $P(EG_{45}$-*b*-$AEMA_{32})$, the selectivity toward HepG2 was dose-dependent on $P(MAGalNAc_{62}$-*b*-$AEMA_{33})$, which further validates the role of GalNAc ligands (Figure S13) in promoting higher efficacy for gene delivery.

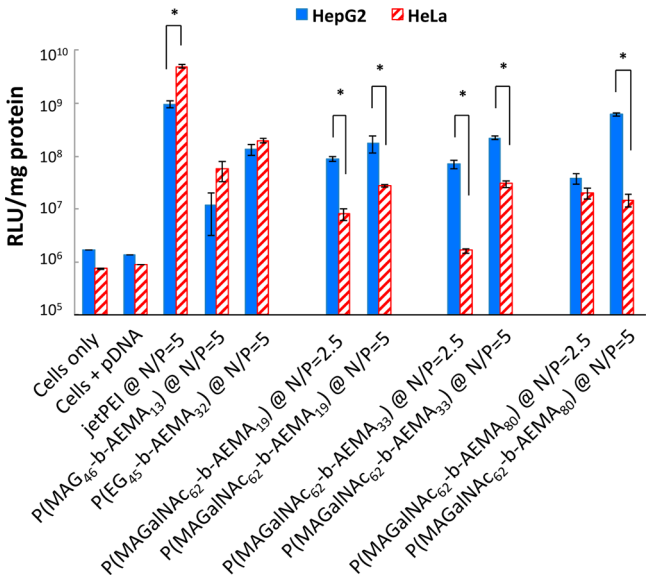

Figure 5. Comparison of luciferase activity in HepG2 (blue, solid fill) and HeLa cells (red, diagonal fill). The luciferase assay was performed 48 h after transfection. Relative light units per mg of protein (RLU/mg protein) are reported as mean ± standard deviation (n = 3). The asterisks indicate statistically different measurements (p < 0.05). The GalNAc-derived polymers show higher gene expression in HepG2 than HeLa, whereas the nontargeted jetPEI, $P(MAG_{46}$-*b*-$AEMA_{13})$, and $P(EG_{45}$-*b*-$AEMA_{32})$ vehicles do not show this preference.

Biodistribution Studies in Mice. Distribution of pDNA and MAGalNAc block copolycations in mice was studied by qPCR and fluorescence imaging, respectively. For qPCR studies, a dose of 40 μg pT2/CAL pDNA was formulated with $P(MAGalNAc_{62}$-*b*-$AEMA_{33})$ at N/P = 2.5 and administered to C57BL/6 mice via tail-vein injection.[29] In vivo-jetPEI was formulated according to manufacturer's recommendation (N/P = 8) and used as a control. The nontargeted $P(MAG_{46}$-*b*-$AEMA_{13})$ polymer was formulated at an N/P of 5 as it showed negligible cellular uptake at lower N/P ratios in previous experiments.[45] At day 1 after systemic administration of polyplexes, mice were euthanized to extract DNA from each tissue. The amount of pDNA in each tissue was determined by quantitative PCR (qPCR) against the luciferase gene on the pT2/CAL plasmid (Figure 6). $P(MAGalNAc_{62}$-*b*-$AEMA_{33})$ formulation at N/P = 2.5 delivered 70-fold higher pDNA to liver as compared to lungs. In contrast, in vivo-jetPEI showed similar levels of pDNA in both of these organs, possibly due to aggregation of nanoparticles following systemic injection leading to the entrapment in lungs after first-pass circulation.[28,29] As a nontargeted control, $P(MAG_{46}$-*b*-$AEMA_{13})$ showed 4 orders of magnitude lower uptake of pDNA in liver compared to $P(MAGalNAc_{62}$-*b*-$AEMA_{33})$ or in vivo-jetPEI. The low amount of pDNA in all tissues is consistent with the low polyplex uptake at an N/P of 5 seen in a previous study,[45] suggesting that this vehicle type circulates well in vivo and discourages nonspecific tissue interactions.

To further understand biodistribution of the polyplexes, $P(MAGalNAc_{62}$-*b*-$AEMA_{33})$ and $P(MAG_{46}$-*b*-$AEMA_{13})$ were labeled with a Cy7 fluorophore, complexed with 40 μg pDNA, and administered to mice via tail-vein injections. The time-course images of fluorescence in whole animal (Figure 7A)

DOI: 10.1021/acs.biomac.5b01555
Biomacromolecules XXXX, XXX, XXX−XXX

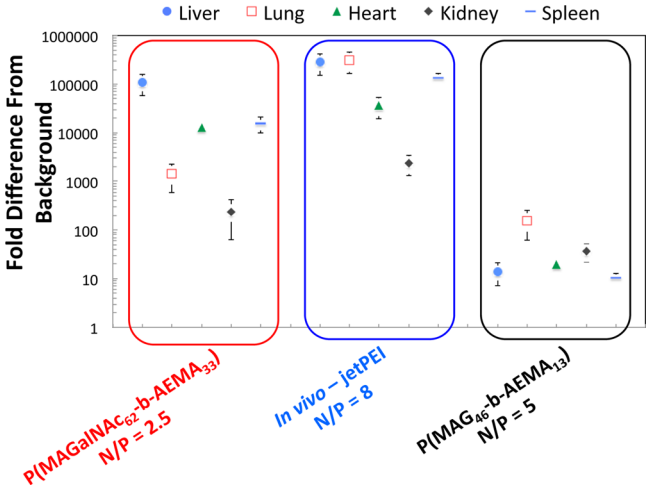

Figure 6. Fold difference from background measured by quantitative polymerase chain reaction against the pT2/CAL plasmid in various tissue samples 1 day following systemic delivery: liver (blue circles), lung (red squares), heart (green triangles), kidney (black diamonds), and spleen (blue horizontal lines). Data are reported as mean ± standard error (n = 3).

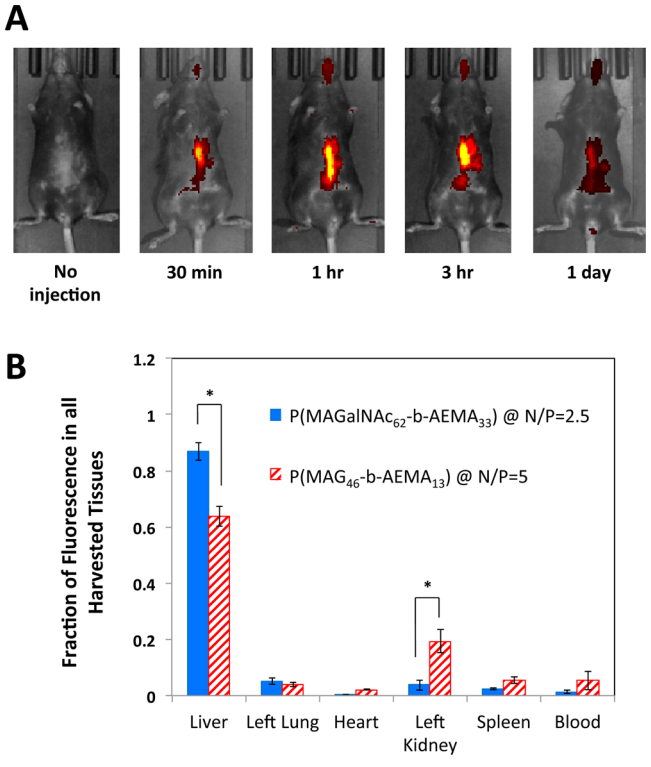

Figure 7. (A) Time-course imaging of fluorescence in live mice after injection of 40 μg pDNA complexed with Cy7-labled P(MAGalNAc$_{62}$-b-AEMA$_{33}$) at N/P = 2.5. (B) Biodistribution of Cy7-labeled P(MAGalNAc$_{62}$-b-AEMA$_{33}$) at N/P = 2.5 (blue, solid fill) and Cy7-labeled P(MAG$_{46}$-b-AEMA$_{13}$) at N/P = 5 (red, diagonal fill) in various tissues, as determined by fluorescence imaging 30 min post-administration. Data are reported as mean ± standard deviation (n = 3). The asterisks (*) indicate that the measurements are statistically different (p < 0.05).

revealed localization of P(MAGalNAc$_{62}$-b-AEMA$_{33}$) to the liver within 30 min post-injection. The highest total fluorescence was seen at 1 h post-injection, whereas the image at 30 min showed the smallest area over which the fluorescence was spread. The decreased fluorescence at 3 h and 1 day post-injection suggests that the polyplexes localize to the liver quickly and are cleared from the body over time. To better understand the biodistribution of polyplexes, individual tissues were harvested 30 min post-injection and imaged to quantify fluorescence intensity (Figure 7). The results for each tissue type are presented in Figure 7B as the fraction of the total measured fluorescence in all harvested tissues. The liver samples were responsible for approximately 80% of the total measured fluorescence from P(MAGalNAc$_{62}$-b-AEMA$_{33}$), whereas the P(MAG$_{46}$-b-AEMA$_{13}$) formulation resulted in a lower amount of polymer in the liver (64% of total fluorescence). The lower amount of P(MAG$_{46}$-b-AEMA$_{13}$) in liver was accounted for by the higher amount present in kidneys (20% of total fluorescence) compared with P(MAGalNAc$_{62}$-b-AEMA$_{33}$) (p < 0.05). Because the MAG block does not interact as strongly with ASGPRs on the liver, P(MAG$_{46}$-b-AEMA$_{13}$) is not sequestered within liver and is excreted through kidney. The higher localization of P(MAGalNAc$_{62}$-b-AEMA$_{33}$) in liver tissue compared to P(MAG$_{46}$-b-AEMA$_{13}$) is in agreement with our hypothesis that GalNAc ligands on the MAGalNAc block facilitate interactions with the ASGPRs on liver cells and therefore provides a novel material for GalNAc-based ASGPR targeting in vivo.

CONCLUSION

We reported the synthesis and polymerization of a novel *N*-acetylgalactosamine-derived monomer (MAGalNAc) that yielded a series of diblock glycopolycations to improve delivery specificity through binding ASGPRs on liver hepatocytes. The MAGalNAc block polycations readily formed polyplexes with pDNA that exhibited higher colloidal stability in cell culture media than polyplexes formed with similar polycations copolymerized from a PEG block. The presence of GalNAc moieties on the polyplexes promoted cell type-dependent delivery, with higher transgene expression in HepG2 (a hepatocyte-derived cell line that displays ASGPRs) as compared to HeLa cells (which lack ASGPRs). Competitive inhibition experiments with HepG2 cells revealed relative binding affinities as follows: PMAGalNAc$_{62}$ ≫ ASF ≫ GalNAc > galactose ≫ glucose. PMAGalNAc$_{62}$ exhibited 2 orders of magnitude higher binding affinity than ASF and five orders higher than monomeric GalNAc, which suggests enhanced binding due to the cluster glycoside effect. Biodistribution experiments in mice revealed a higher amount of pDNA in liver as compared to lungs and other organs when delivered with P(MAGalNAc$_{62}$-b-AEMA$_{33}$) at N/P = 2.5. Nontargeted in vivo-jetPEI showed higher lung uptake in comparison and P(MAG$_{46}$-b-AEMA$_{13}$) showed low internalization by all tissues. In addition, Cy7-labeled P(MAGalNAc$_{62}$-b-AEMA$_{33}$) revealed a higher fraction of polymer localization to the liver as compared to the nontargeted P(MAG$_{46}$-b-AEMA$_{13}$) control. This study offers a facile design motif for functionalizing nanomedicines to enhance delivery specificity to the liver, an organ of wide interest for drug, siRNA, and gene therapy/genome editing applications. Further investigation of the effect of blood components on these polyplexes, kinetics of their systemic distribution, localization at the cellular level within the liver, and immunogenicity are in progress and are expected to provide useful fundamental insights to guide the future design of efficacious targeted delivery vehicles.

DOI: 10.1021/acs.biomac.5b01555
Biomacromolecules XXXX, XXX, XXX−XXX

■ ASSOCIATED CONTENT

Supporting Information

The Supporting Information is available free of charge on the ACS Publications website at DOI: 10.1021/acs.biomac.5b01555.

NMR spectra and SEC traces of polymers synthesized in this study, gel electrophoresis of polyplexes, and additional cell culture experiments (PDF).

■ AUTHOR INFORMATION

Corresponding Author

*E-mail: treineke@umn.edu.

Notes

The authors declare no competing financial interest.

■ ACKNOWLEDGMENTS

We acknowledge the University of Minnesota and the National Institutes of Health (NIH 1DP2 OD00666901, NIH/NIDDK 5R01-DK082516, NIH/NICHD 5P01-HD032652) for funding this work and the University of Minnesota Genomics Center for running quantitative polymerase chain reactions.

■ REFERENCES

(1) Follenzi, A.; Battaglia, M.; Lombardo, A.; Annoni, A.; Roncarolo, M. G.; Naldini, L. *Blood* **2004**, *103* (10), 3700−3709.

(2) Park, J. W.; Hong, K.; Kirpotin, D. B.; Colbern, G.; Shalaby, R.; Baselga, J.; Shao, Y.; Nielsen, U. B.; Marks, J. D.; Moore, D.; Papahadjopoulos, D.; Benz, C. C. *Clin. Cancer Res.* **2002**, *8* (4), 1172−1181.

(3) Panyam, J.; Labhasetwar, V. *Adv. Drug Delivery Rev.* **2003**, *55* (3), 329−347.

(4) European Medicines Agency, *Glybera-EPAR Summary for the Public,* 2012

(5) Ginn, S. L.; Alexander, I. E.; Edelstein, M. L.; Abedi, M. R.; Wixon, J. *J. Gene Med.* **2013**, *15* (2), 65−77.

(6) Naldini, L. *Nature* **2015**, *526* (7573), 351−360.

(7) Cheung, S. T.; Tsui, T. Y.; Wang, W. L.; Yang, Z. F.; Wong, S. Y.; Ip, Y. C.; Luk, J.; Fan, S. T. *J. Gastroenterol. Hepatol.* **2002**, *17* (9), 1008−1014.

(8) High, K. H.; Nathwani, A.; Spencer, T.; Lillicrap, D. *Haemophilia* **2014**, *20* (s4), 43−49.

(9) Mátrai, J.; Chuah, M. K.; VandenDriessche, T. *Curr. Opin. Hematol.* **2010**, *17* (5), 387−392.

(10) Ponder, K. P. *Mol. Ther.* **2011**, *19* (3), 427−428.

(11) Sands, M. S.; Davidson, B. L. *Mol. Ther.* **2006**, *13* (5), 839−849.

(12) Cheng, S. H.; Smith, A. E. *Gene Ther.* **2003**, *10* (16), 1275−1281.

(13) Nair, J. K.; Willoughby, J. L. S.; Chan, A.; Charisse, K.; Alam, M. R.; Wang, Q.; Hoekstra, M.; Kandasamy, P.; Kel'in, A. V.; Milstein, S.; Taneja, N.; O'Shea, J.; Shaikh, S.; Zhang, L.; van der Sluis, R. J.; Jung, M. E.; Akinc, A.; Hutabarat, R.; Kuchimanchi, S.; Fitzgerald, K.; Zimmermann, T.; van Berkel, T. J. C.; Maier, M. A.; Rajeev, K. G.; Manoharan, M. *J. Am. Chem. Soc.* **2014**, *136* (49), 16958−16961.

(14) Hu, Y.; Haynes, M. T.; Wang, Y.; Liu, F.; Huang, L. *ACS Nano* **2013**, *7* (6), 5376−5384.

(15) Thomas, M.; Klibanov, A. M. *Appl. Microbiol. Biotechnol.* **2003**, *62* (1), 27−34.

(16) Morille, M.; Passirani, C.; Vonarbourg, A.; Clavreul, A.; Benoit, J.-P. *Biomaterials* **2008**, *29* (24), 3477−3496.

(17) Fischer, D.; Bieber, T.; Li, Y.; Elsässer, H.-P.; Kissel, T. *Pharm. Res.* **1999**, *16* (8), 1273−1279.

(18) Kwoh, D. Y.; Coffin, C. C.; Lollo, C. P.; Jovenal, J.; Banaszczyk, M. G.; Mullen, P.; Phillips, A.; Amini, A.; Fabrycki, J.; Bartholomew, R. M.; Brostoff, S. W.; Carlo, D. J. *Biochim. Biophys. Acta, Gene Struct. Expression* **1999**, *1444* (2), 171−190.

(19) van de Wetering, P.; Cherng, J.-Y.; Talsma, H.; Hennink, W. E. *J. Controlled Release* **1997**, *49* (1), 59−69.

(20) Verbaan, F.; van Dam, I.; Takakura, Y.; Hashida, M.; Hennink, W.; Storm, G.; Oussoren, C. *Eur. J. Pharm. Sci.* **2003**, *20* (4−5), 419−427.

(21) Wu, Y.; Wang, M.; Sprouse, D.; Smith, A. E.; Reineke, T. M. *Biomacromolecules* **2014**, *15* (5), 1716−1726.

(22) Rejman, J.; Conese, M.; Hoekstra, D. *J. Liposome Res.* **2006**, *16* (3), 237−247.

(23) von Gersdorff, K.; Sanders, N. N.; Vandenbroucke, R.; De Smedt, S. C.; Wagner, E.; Ogris, M. *Mol. Ther.* **2006**, *14* (5), 745−753.

(24) McLendon, P. M.; Fichter, K. M.; Reineke, T. M. *Mol. Pharmaceutics* **2010**, *7* (3), 738−750.

(25) Ingle, N. P.; Xue, L.; Reineke, T. M. *Mol. Pharmaceutics* **2013**, *10* (11), 4120−4135.

(26) Pack, D. W.; Hoffman, A. S.; Pun, S.; Stayton, P. S. *Nat. Rev. Drug Discovery* **2005**, *4* (7), 581−593.

(27) Smith, A. E.; Sizovs, A.; Grandinetti, G.; Xue, L.; Reineke, T. M. *Biomacromolecules* **2011**, *12* (8), 3015−3022.

(28) Sharma, V. K.; Thomas, M.; Klibanov, A. M. *Biotechnol. Bioeng.* **2005**, *90* (5), 614−620.

(29) Podetz-Pedersen, K. M.; Bell, J. B.; Steele, T. W.; Wilber, A.; Shier, W. T.; Belur, L. R.; McIvor, R. S.; Hackett, P. B. *Hum. Gene Ther.* **2010**, *21* (2), 210−220.

(30) Oupicky, D.; Ogris, M.; Howard, K. A.; Dash, P. R.; Ulbrich, K.; Seymour, L. W. *Mol. Ther.* **2002**, *5* (4), 463−472.

(31) Dash, P. R.; Read, M. L.; Barrett, L. B.; Wolfert, M. A.; Seymour, L. W. *Gene Ther.* **1999**, *6* (4), 643−650.

(32) Ogris, M.; Brunner, S.; Schüller, S.; Kircheis, R.; Wagner, E. *Gene Ther.* **1999**, *6* (4), 595−605.

(33) Verbaan, F. J.; Oussoren, C.; Snel, C. J.; Crommelin, D.; Hennink, W. E.; Storm, G. *J. Gene Med.* **2004**, *6* (1), 64−75.

(34) Ishihara, T.; Takeda, M.; Sakamoto, H.; Kimoto, A.; Kobayashi, C.; Takasaki, N.; Yuki, K.; Tanaka, K.-I.; Takenaga, M.; Igarashi, R.; Maeda, T.; Yamakawa, N.; Okamoto, Y.; Otsuka, M.; Ishida, T.; Kiwada, H.; Mizushima, Y.; Mizushima, T. *Pharm. Res.* **2009**, *26* (10), 2270−2279.

(35) Tagami, T.; Uehara, Y.; Moriyoshi, N.; Ishida, T.; Kiwada, H. *J. Controlled Release* **2011**, *151* (2), 149−154.

(36) Samsonova, O.; Pfeiffer, C.; Hellmund, M.; Merkel, O. M.; Kissel, T. *Polymers* **2011**, *3* (2), 693−718.

(37) Johnson, R. P.; Uthaman, S.; John, J. V.; Heo, M. S.; Park, I. K.; Suh, H.; Kim, I. *Macromol. Biosci.* **2014**, *14* (9), 1239−1248.

(38) Wen, Y.; Zhang, Z.; Li, J. *Adv. Funct. Mater.* **2014**, *24* (25), 3874−3884.

(39) Dai, F.; Liu, W. *Biomaterials* **2011**, *32* (2), 628−638.

(40) Liang, G. F.; Zhu, Y. L.; Sun, B.; Hu, F. H.; Tian, T.; Li, S. C.; Xiao, Z. D. *Nanoscale Res. Lett.* **2011**, *6* (447), 1−9.

(41) Mishra, D.; Kang, H. C.; Bae, Y. H. *Biomaterials* **2011**, *32* (15), 3845−3854.

(42) Sizovs, A.; Xue, L.; Tolstyka, Z. P.; Ingle, N. P.; Wu, Y.; Cortez, M.; Reineke, T. M. *J. Am. Chem. Soc.* **2013**, *135* (41), 15417−15424.

(43) Li, H.; Cortez, M. A.; Phillips, H. R.; Wu, Y.; Reineke, T. M. *ACS Macro Lett.* **2013**, *2* (3), 230−235.

(44) Buckwalter, D. J.; Sizovs, A.; Ingle, N. P.; Reineke, T. M. *ACS Macro Lett.* **2012**, *1* (5), 609−613.

(45) Sprouse, D.; Reineke, T. M. *Biomacromolecules* **2014**, *15* (7), 2616−2628.

(46) Hashida, M.; Takemura, S.; Nishikawa, M.; Takakura, Y. *J. Controlled Release* **1998**, *53* (1−3), 301−310.

(47) Wang, H.-X.; Xiong, M.-H.; Wang, Y.-C.; Zhu, J.; Wang, J. *J. Controlled Release* **2013**, *166* (2), 106−114.

(48) Prakash, T. P.; Graham, M. J.; Yu, J.; Carty, R.; Low, A.; Chappell, A.; Schmidt, K.; Zhao, C.; Aghajan, M.; Murray, H. F.; Riney, S.; Booten, S. L.; Murray, S. F.; Gaus, H.; Crosby, J.; Lima, W. F.; Guo, S.; Monia, B. P.; Swayze, E. E.; Seth, P. P. *Nucleic Acids Res.* **2014**, *42* (13), 8796−8807.

(49) Tang, L.; Wu, Y.; Lu, J.; Zhang, Z. R.; Yang, J. C.; Hai, L. *Chin. Chem. Lett.* **2007**, *18* (5), 513−515.

DOI: 10.1021/acs.biomac.5b01555
Biomacromolecules XXXX, XXX, XXX−XXX

(50) Lee, R. T.; Lee, Y. C. *Glycoconjugate J.* **2000**, *17* (7−9), 543−551.
(51) Khorev, O.; Stokmaier, D.; Schwardt, O.; Cutting, B.; Ernst, B. *Bioorg. Med. Chem.* **2008**, *16* (9), 5216−5231.
(52) Shen, Z.; Wei, W.; Tanaka, H.; Kohama, K.; Ma, G.; Dobashi, T.; Maki, Y.; Wang, H.; Bi, J.; Dai, S. *Pharmacol. Res.* **2011**, *64* (4), 410−419.
(53) Thapa, B.; Kumar, P.; Zeng, H.; Narain, R. *Biomacromolecules* **2015**, *16* (9), 3008−3020.
(54) Rensen, P. C. N.; van Leeuwen, S. H.; Sliedregt, L. A. J. M.; van Berkel, T. J. C.; Biessen, E. A. L. *J. Med. Chem.* **2004**, *47* (23), 5798−5808.
(55) Xu, X.; Smith, A. E.; Kirkland, S. E.; McCormick, C. L. *Macromolecules* **2008**, *41* (22), 8429−8435.
(56) Gesztelyi, R.; Zsuga, J.; Kemeny-Beke, A.; Varga, B.; Juhasz, B.; Tosaki, A. *Arch. Hist. Exact Sci.* **2012**, *66* (4), 427−438.
(57) Moad, G.; Rizzardo, E.; Thang, S. H. *Chem. - Asian J.* **2013**, *8*, 1634−1644.
(58) Pujol, A. M.; Cuillel, M.; Jullien, A. S.; Lebrun, C.; Cassio, D.; Mintz, E.; Gateau, C.; Delangle, P. *Angew. Chem.* **2012**, *124* (30), 7563−7566.
(59) Kallinteri, P.; Papadimitriou, E.; Antimisiaris, S. G. *J. Liposome Res.* **2001**, *11* (2−3), 175−193.
(60) Tanaka, T.; Abo, Y.; Hamano, S.; Fujishima, Y.; Kaneo, Y. *J. Drug Delivery Sci. Technol.* **2013**, *23* (5), 435−438.
(61) Detampel, P.; Witzigmann, D.; Krähenbühl, S.; Huwyler, J. *J. Drug Target* **2013**, *22* (3), 232−241.
(62) Yet, M. G.; Chin, C.; Wold, F. *J. Biol. Chem.* **1988**, *263* (1), 111−117.
(63) Kim, S.-H.; Goto, M.; Akaike, T. *J. Biol. Chem.* **2001**, *276* (38), 35312−35319.
(64) Mamidyala, S. K.; Dutta, S.; Chrunyk, B. A.; Préville, C.; Wang, H.; Withka, J. M.; McColl, A.; Subashi, T. A.; Hawrylik, S. J.; Griffor, M. C.; Kim, S.; Pfefferkorn, J. A.; Price, D. A.; Menhaji-Klotz, E.; Mascitti, V.; Finn, M. G. *J. Am. Chem. Soc.* **2012**, *134* (4), 1978−1981.
(65) Zhang, X. R.; Jia, J. L.; Zhang, R. J.; Xu, M. H.; Zhang, S. S. *Chin. J. Chem.* **2006**, *24* (8), 1058−1061.
(66) Westerlind, U.; Westman, J.; Tornquist, E.; Smith, C.; Oscarson, S.; Lahmann, M.; Norberg, T. *Glycoconjugate J.* **2004**, *21* (5), 227−241.
(67) Lundquist, J. J.; Toone, E. J. *Chem. Rev.* **2002**, *102* (2), 555−578.
(68) Li, Y.; Huang, G.; Diakur, J.; Wiebe, L. I. *Curr. Drug Delivery* **2008**, *5* (4), 299−302.
(69) Anderson, K.; Sizovs, A.; Cortez, M.; Waldron, C.; Haddleton, D. M.; Reineke, T. M. *Biomacromolecules* **2012**, *13* (8), 2229−2239.
(70) Dai, Z.; Gjetting, T.; Mattebjerg, M. A.; Wu, C.; Andresen, T. L. *Biomaterials* **2011**, *32* (33), 8626−8634.
(71) Xu, T.; Liu, W.; Wang, S.; Shao, Z. *Int. J. Nanomed.* **2014**, *9* (1), 3231−3245.

DOI: 10.1021/acs.biomac.5b01555
Biomacromolecules XXXX, XXX, XXX−XXX